Available online at www.sciencedirect.com

ScienceDirect

Proceedings of the Combustion Institute 37 (2019) 4053–4061

Proceedings of the Combustion Institute

www.elsevier.com/locate/proci

The effect of chemical composition on the charring of wood across scales

Franz Richter [a], Arvind Atreya [b], Panagiotis Kotsovinos [c], Guillermo Rein [a,*]

[a] *Department of Mechanical Engineering, Imperial College London, London, UK*
[b] *Department of Mechanical Engineering, University of Michigan, Ann Arbor, USA*
[c] *Arup, Manchester, UK*

Received 30 November 2017; accepted 11 June 2018
Available online 6 July 2018

Abstract

Structural softwood (timber) recently gained attention by architects and engineers as a construction material for high-rise buildings. Regulations restrict the height of these buildings due to safety concerns as their fire behaviour is poorly understood. The fire behaviour and loss of loadbearing capacity of timber is controlled by charring, whose chemical kinetics has rarely been studied. Current models of charring assume, without proof, the same reaction scheme and kinetic parameters apply to all wood species, which potentially introduces a large uncertainty. Here, the hypothesis is tested that the kinetics of different wood species insignificantly affects their charring behaviour. The kinetics is modelled by a microscale kinetic model—including pyrolysis and char oxidation reactions—which assumes that the three main components (cellulose, hemicellulose, and lignin) of wood degrade independently. Variation in the kinetics between different wood species is captured by their different chemical compositions within a wood group (softwood or hardwood). Hardwood is included for comparison. A database of over 600 compositions was compiled from literature, and studied across scales using a microscale (mg-samples) and mesoscale (kg-samples) model. All reactions, kinetic parameters, and physical properties were selected from literature. Both models were validated using blind predictions of high-fidelity experiments from literature. Variation in kinetics were found to have a small effect on the predicted mass loss rate at both scales (± 1 g/m^2-s) and a negligible effect on the predicted temperatures (± 16 K) across different depths, heat fluxes, and oxygen concentrations at the mesoscale. These results prove, for the first time, that the variation in kinetics is negligible for predicting charring across scales. A kinetic model of charring derived for one wood species should be valid for all wood species within softwood or hardwood. Modellers should, therefore, focus on the difference in the physical properties instead of the kinetics between wood species.

Keywords: Timber; Fire; Pyrolysis; Kinetics; Oxidation

* Corresponding author.
E-mail address: g.rein@imperial.ac.uk (G. Rein).

https://doi.org/10.1016/j.proci.2018.06.080

Nomenclature

A	pre-exponential factor
c	heat capacity
E	activation energy
h	enthalpy
h_c	convective coefficient
ΔH	heat of reaction
k	thermal conductivity
K	permeability
$\dot{m}''$	mass flux
n	reaction order
P	pressure
$\dot{q}''_e$	external heat flux
$\dot{q}''_r$	radiative heat flux
t	time
T	temperature
Y	mass fraction
Z	distance
n_{O_2}	oxygen reaction order

Greeks

E	Emissivity
K	Radiative absorption coefficient
ρ	Bulk density
ν	Viscosity or solid yield
ρ_s	Density of condensed species
Φ	Porosity
$\dot{\omega}'''$	Volumetric reaction rate

Subscripts

d	Destruction
f	Formation
g	Gas
i	Condensed species index
j	Gaseous species index
k	Reaction index

1. Introduction

Wood is an ancient material, traditionally used as fuel, furniture, or construction material for low-rise buildings. Only recently has structural softwood (timber) gained attention as a construction material for high-rise buildings [1], because it is strong, sustainable, and cost-efficient. In fact, timber is made environmentally sustainable by nature. In nature, the stem holds the crown of a tree up to 100-m-high, just like a timber column could hold a building over 100-m-high. The lack of knowledge of the fire behaviour of timber, however, has led authorities to restrict the height of timber buildings to mid-rise around the world for safety concerns.

Charring (pyrolysis and heterogeneous oxidation) control the burning behaviour of wood. For example, the loss of structural loadbearing capacity of timber (softwood) during a fire is determined by the charring rate, which for the lack of knowledge is often assumed constant under all conditions. Previous works studied the influence of heat flux, density, and oxygen concentration on charring [2–6]. Variation in the charring rate of different wood species was believed to be explained by different material properties [2]. This assumption implies that charring is dominated by heat transfer, but both heat transfer and kinetics control charring [6]. Mueller-Hagedorn et al. [7] showed that different wood species have different kinetics at the microscale, which are dictated by their chemical composition. One only has to divide wood into softwood (coniferous trees) and hardwood (deciduous trees). The importance of these differences for charring at the large scale remains unknown. Here, we test the hypothesis that the kinetics of different wood species insignificantly affects their charring behaviour.

Based on previous work [7–9], we express the difference in kinetics between wood species by one kinetic model with different chemical compositions. To predict the behaviour at different scales, we examine the kinetics at both the micro and mescoscale. At the microscale (mg-samples), we study the effect of varying the chemical composition on the kinetics of thermal degradation. At the mesoscale (kg-samples), we then study the effect on kinetics, heat transfer, and mass transfer. These results are disussed for softwood (timber) with hardwood presented for comparison. Based on these results, the importance of different kinetics for structural timber members in buildings (macroscale) is discussed.

2. Methods

2.1. Mircoscale model

The kinetics of wood is measured at the microscale with mg-samples in a small furnace (TGA) at a constant heating rate. In this study, the reaction scheme and kinetic parameters are taken from and verified (see supplementary materials Fig. S1) against [8]. They predict the ignition of timber satisfactorily [10]. Wood pyrolysis is modelled as the linear superposition of its three main components: cellulose, hemicellulose and lignin. The initial mass fraction of each component is given by the chemical composition of the wood. Each component is assumed to yield the same char and follow independently the same reaction scheme shown in Fig. 1.

We added a char oxidation reaction (R4) to the pyrolysis scheme, as it was observed in the mesoscale experiments [11] and is necessary for accurate predictions [5]. We used the kinetic parameters by Kashiwagi and Nambu [12] for R4, taking cellulose char as a surrogate for wood char. In total, there are 10 reactions and 10 species. The model presented focusses on charring: only non-flaming experiments were considered (without combustion reactions in the gas-phase). The

Table 1
Kinetic parameters in the format of E / log A / ν / ΔH in the units of (kJ/mol) / (log s^{-1}) / (-) / (kJ/g).

Reaction	R1	R2	R3	R4, char to ash
Cellulose	242/19.4/1/0	197/14.5/0/0.26	151/10.1/0.35/0	160/9.75/0.03/−11.9
Hemicellulose	186/16.3/1/0	202/15.9/0/0.26	145/11.4/0.62/0	
Lignin	107/8.98/1/0	144/9.18/0/0.26	111/6.89/0.75/0	

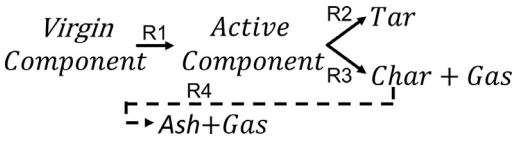

Fig. 1. Reaction scheme of each component. Where (—) are pyrolysis reactions and (- -) are oxidation reactions.

rate of the pyrolysis and oxidation reactions is described by Eq. (1) with all kinetic parameters given in Table 1.

$$\dot{\omega}_i''' = \bar{\rho} Y_{A,k} Y_{O_2}^{n_{O_2 k}} A_k \exp(-E_k/RT) \quad (1)$$

The order of oxidation (n_{O_2}) is zero for pyrolysis [8] and 0.78 for oxidation reactions [12]. The heat of reaction for each pyrolysis reaction (R1 to R3) is from [10] and for the char oxidation reaction (R4) from [13].

2.2. Mesoscale model

At the mesoscale the in-depth temperatures and mass loss rates of kg-samples are measured [2]. The model is similar to [10], which solves 6 conservation equations: those for the condensed-phase mass (2), species (3), and energy (4), and those for the gas-phase mass (5), species (6), and momentum (7).

$$\frac{\partial \bar{\rho}}{\partial t} = -\dot{\omega}_{fg}''' \quad (2)$$

$$\frac{\partial (\overline{\rho Y_i})}{\partial t} = \dot{\omega}_{fi}''' - \dot{\omega}_{di}''' \quad (3)$$

$$\frac{\partial (\bar{\rho}\bar{h})}{\partial t} = \frac{\partial}{\partial z}\left(\bar{k}\frac{\partial T}{\partial z}\right) + \sum_{i=1}^{K} \dot{\omega}_{fi}'''(-\Delta H_i) - \frac{\partial \dot{q}_r''}{\partial z} \quad (4)$$

$$\frac{\partial}{\partial t}(\rho_g \bar{\phi}) + \frac{\partial \dot{m}''}{\partial z} = \dot{\omega}_{fg}''' \quad (5)$$

$$\frac{\partial}{\partial t}(\rho_g \bar{\phi} Y_j) + \frac{\partial}{\partial z}(\dot{m}'' Y_j) = -\frac{\partial}{\partial z}\left(\bar{\phi}\rho_g D \frac{\partial Y_j}{\partial z}\right) + \dot{\omega}_{fj}''' - \dot{\omega}_{dj}''' \quad (6)$$

$$\dot{m}'' = -\frac{K}{\nu}\frac{\partial p}{\partial z} \quad (7)$$

$$\dot{q}_r'' = \bar{\varepsilon}\dot{q}_e'' e^{-\bar{\kappa} z}. \quad (8)$$

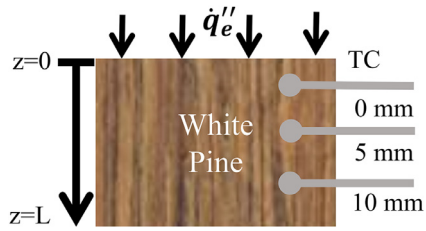

Fig. 2. Experimental and computational set-up to study charring. TC—thermal-couple position.

All properties in Eqs. (2)–(8) are averaged (overbar) based on mass or volume fraction. We assume thermal equilibrium between the gas and solid phases, and Darcy flow within the porous solid. Figure 2 illustrates the computational domain. Convection, re-radiation, and incident heat flux are modelled at the free surface (z = 0), while only convection is modelled at the back surface (z = 38 mm) where the temperature rise is small, around 50°C [14]. The values of the convection coefficients are from [3]. The free surface allows diffusion of gaseous species, while the back surface is impermeable. We also assume negligible heat losses to the lateral sides. Furthermore, the model includes surface regression (see [15] for details) and in-depth radiation (Eq. (8)). The conservation Eq. (1)–(8), together with the boundary and initial conditions were solved fully implicitly in Gpyro 0.700, with further details provided elsewhere [3]. A time-step of 0.1 s and a cell size of $\Delta z = 0.05$ mm ensured convergence in all simulations. In comparison to [10], we simulated different experiments, incorporated oxidation into the kinetics (Section 2.1), and corrected the material properties of the wood (Table 2).

All material properties (Table 2) are taken from literature and assumed to be temperature independent. They were either measured by Ohlemiller et al. [11,14] or selected from the literature, following a literature review, based on their quality, use in modelling, and similarity to the studied species. Following others [8], the virgin and active components of cellulose, hemicellulose and lignin have the same material properties as wood (here timber). The density and emissivity of timber were measured and estimated in the experiments [11,14]. All other material properties of timber and char are from [10], and for ash from [16]. The density of char was changed to a plausible value for the stud-

Table 2
Material properties of each species from [4,10,16]. * measured or estimated by Ohlemiller et al. [11,14].

Species	ρ (kg/m^3)	k (W/m-K)	c (J/kg-K)	ϵ(-)	κ (m^{-1})	ρ_s (kg/m^3)
Timber	380*	0.126	2300	0.7*	570	2167
Char	162	0.084	1100	0.95	570	2333
Ash	19.5	0.8	880	0.95	∞	2500

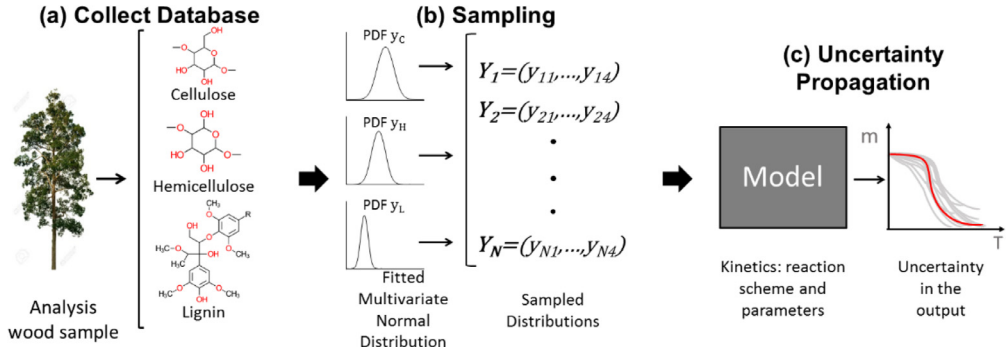

Fig. 3. Flow chart of the propagation of chemical composition, treated as an uncertain parameter, through the microscale model. m is the residual mass and T is the temperature. Molecular structures are from [9].

ied species (380 kg/m^3) from 330 [10] to 162 kg/m^3 [4].

2.3. Database of chemical composition and propagation of uncertainty

The wood species used in the initial design and construction of a building can differ, and it is important to quantify this uncertainty. Figure 3 illustrates the used methodology of uncertainty propagation, where uncertain parameters are treated as random variables with a defined probability distribution. We propagated the distributions of uncertain input parameters (mass fraction of each component in the composition) through a model with a large number of simulations, where the uncertain parameters were drawn randomly from their distributions (Monte Carlo). From these simulations the probability distribution (uncertainty) of the output was built.

To derive the input probability distribution, over 600 chemical compositions of wood species from the literature (see supplementary material Table S1) were compiled into one database. This database was split into two groups according to the tree's reproduction: one for softwood and one for hardwood. Softwood is used for construction (timber) and hardwood mainly for energy. They are separated as they behave differently (see Section 3.1 or [7]). A multi-variant normal distribution was fitted to each group. The fitted distribution was verified by comparison of its probability density function, cumulative density function, and covariance matrix with the original data. We applied this methodology to the microscale (1000 samples) and mesoscale (500 samples) model.

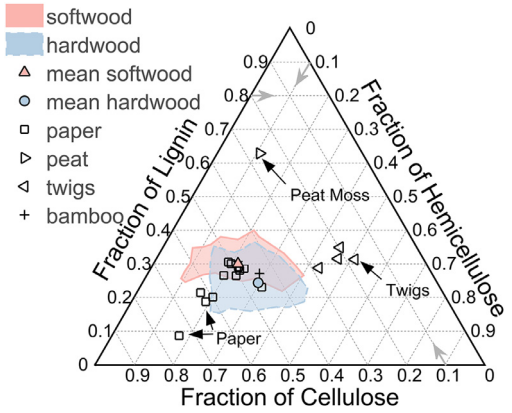

Fig. 4. Ternary plot of all compositions of softwood and hardwood reported in the database (see supplementary material Table S1). For comparison paper, peat, and twigs [18] are shown.

3. Results and discussion

3.1. Variation of chemical composition

The mass fraction of each component between stem wood and other biomass differs significantly (Fig. 4). For example, the mass fraction of hemicellulose and lignin only varies between 0.1 and 0.44 in stem wood, while higher val-

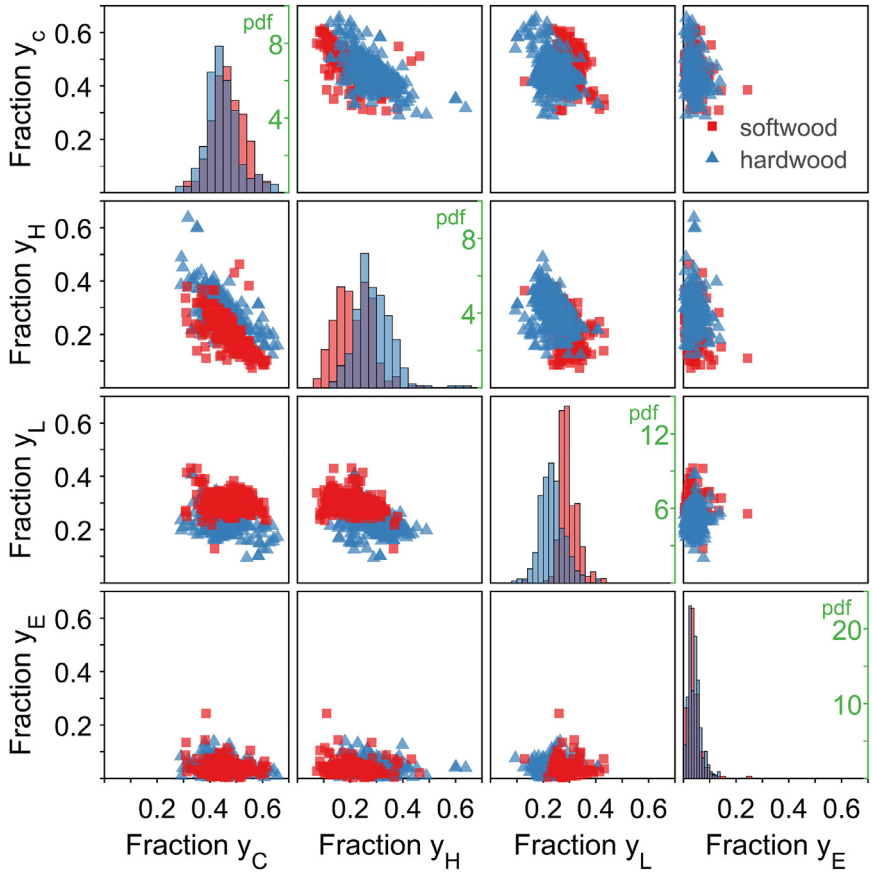

Fig. 5. Covariance between the different fraction of softwood (■ red) and hardwood (▲blue)—cellulose y_C, hemicellulose y_H, lignin y_L, and extractives y_E. The diagonal shows the histogram of each component with the green y-axis showing the height of the probability density function (pdf). (For interpretation of the references to color in this figure legend, the reader is referred to the web version of this article.)

ues can be found for peat and twigs. Within wood the composition of softwood and hardwood differ. Softwood shows on average a greater content of cellulose (47 vs 46%) and lignin (29 vs 23%) than hardwood. Its hemicellulose contains mainly mannans, while hardwood contains mainly xylan [7]. These differences cause different mass loss rates at the microscale [7], and the two are, therefore, analysed separately [7,17].

The diagonal of Fig. 5 illustrates the histograms of the components of softwood and hardwood. All components are approximately normally distributed as indicated by the Kolmogorov-Smirnov test (average p-value: 0.26). All other graphs in Fig. 5 show the fraction of one component plotted against another (covariance). Cellulose and hemicellulose are strongly correlated while the other components are mostly moderately correlated (see supplementary material Table S2). The covariance between components is, therefore, significant which supports our choice of using a multivariate normal distribution for the input parameters in the uncertainty propagation (Section 2.3). As the average fraction of extractives in wood is below 5% and extractives decompose at similar temperatures to hemicellulose [19], the assumption of adding them to hemicellulose [8] is reasonable.

3.2. *Effect of chemical composition at the microscale*

Fig. 6 compares the predicted residual mass and reaction rate (normalised mass loss rate) of the microscale model for softwood (a and b) and hardwood (c and d) with state-of-the-art experiments [20]. The shaded region represents the variability in the predictions from the Monte-Carlo simulations. Darker shading represents a higher probability of obtaining a prediction in that region, with the black lines showing the average.

For softwood, the kinetics predicts the residual mass within the experimental uncertainty (Fig. 6a),

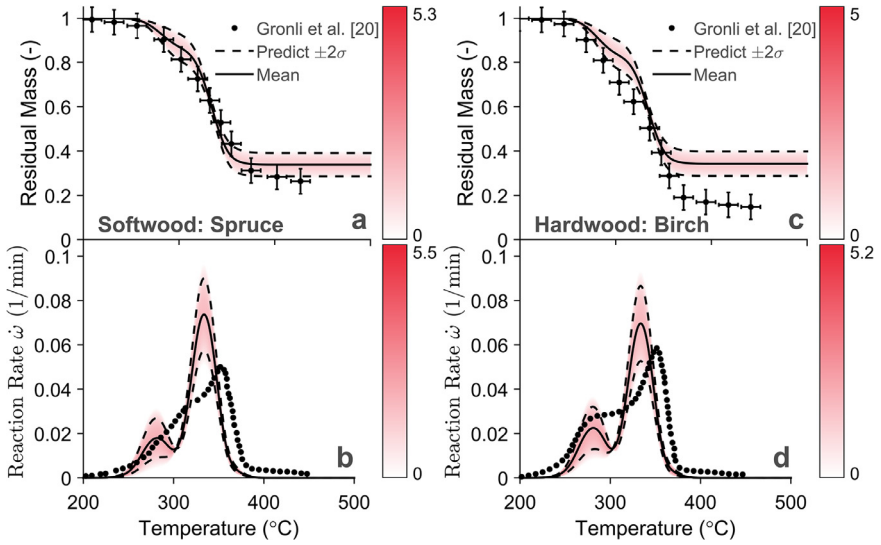

Fig. 6. Comparison between kinetic model and experiments—state-of-the-art experiments by Gronli et al. [20] of two commonly used species—at the microscale at 5 K/min in inert environment. The shadow area represents the log probability density obtained from the Monte-Carlo simulations.

but the reaction rate is shifted to lower temperatures than in the experiments (Fig. 6b). Predictions show two peaks, but the peak at 280°C is experimentally only observed for hardwood, as it stems from the degradation of xylan (hardwoods hemicellulose) [7]. These discrepancies between hardwood and softwood are discussed in [7,17] and between the predictions and the hardwood experiments (Fig. 6d) in [8], where the latter were judged acceptable. As the agreement between the predictions and the softwood experiments is similar to that of hardwood (see Fig. 6), they can also be judged acceptable.

Different species—expressed by different chemical composition—degrade similar and yield similar residual mass histories (Fig. 6a). The probability density function of the component's mass fractions and the predicted reaction rate are also the same (Fig. 6b). They both have the same distribution (normal) and a similar standard deviation (13 and 22% respectively). As the variation in the chemical composition of softwood is small, the variation in height and location of the reaction rate peak is small and none respectively. The same argument holds for hardwood (Fig. 6c and d). The difference in kinetics within hardwood and softwood is, therefore, negligible at the microscale for the charring of wood.

Gronli et al. [20] found experimentally small differences in the reaction rate within common softwoods and hardwoods. From these results, Anca-Couce and Obernberger [17] concluded that only one composition for hardwood and softwood respectively is necessary to predict pyrolysis at the microscale, which is consistent with our findings. Their proposed compositions are also close to the average compositions found here (Table 3).

3.3. Effect of chemical composition at the mesoscale

Figs. 7 and 8 show the comparison between predictions of the mesoscale model and the experiments of [11,14] at two different heat fluxes and different oxygen concentrations. All predictions are blind.

At both heat fluxes, the model shows good agreement with all temperatures, regardless of the composition (Figs. 7a–c and 8a). The average error in the temperatures (37 K) is close to a conservative estimated experimental error of ± 30 K based on [21]. Only the surface temperatures show some discrepancies which are insignificant, because charring rates are determined from in-depth temperature profiles and not surface temperatures.

On the other hand, the average error across all data points of the mass loss rate (34%) is significantly worse than for the temperatures (15%). Qualitatively the model reproduces the experiments. It shows one sharp peak for the case of 40 kW/m^2 (Fig. 7d) and a delayed peak for the case of 25 kW/m^2 (Fig. 8a). However, the peaks are predicted too early at both heat fluxes and are too high at 40 kW/m^2, and too low at 25 kW/m^2.

These disagreements are consistent with studies from several state-of-the-art pyrolysis models of polymers [22]. They found discrepancies with the mass loss rate appear when using incomplete kinetics or neglecting the heat of pyrolysis [22]. As the predictions of the temperatures are good, the heat of pyrolysis is an unlikely cause for the dis-

Table 3
Comparison between measured and proposed composition of softwood and hardwood in the literature [17].

	Cellulose (%)		Hemicellulose (%)		Lignin (%)		Extractives (%)	
	[17]	Mean	[17]	Mean	[17]	Mean	[17]	Mean
Hardwood	44	45 ± 6	34	29 ± 7	22	23 ± 5	0	4.2 ± 2.4
Softwood	44	47 ± 6	26	21 ± 7	30	29 ± 5	0	3.9 ± 2.9

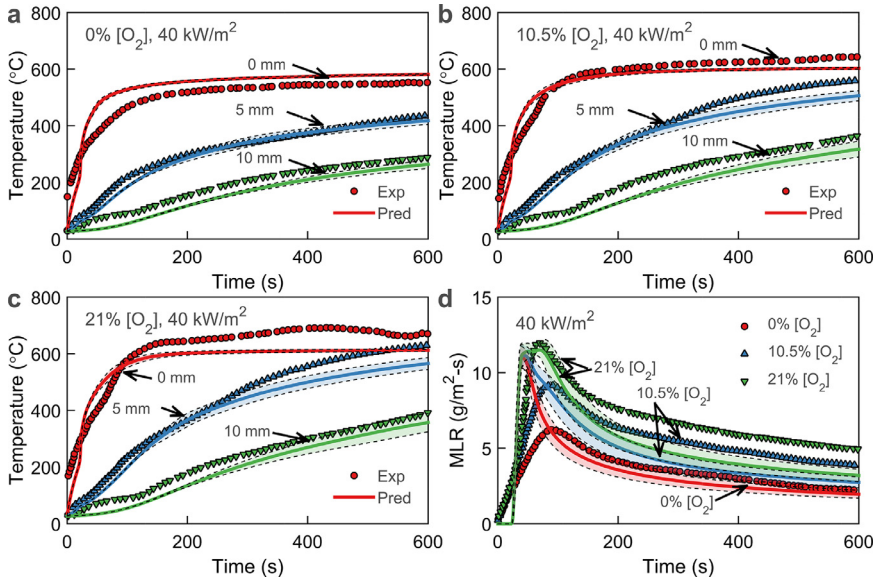

Fig. 7. Comparison between the predictions (lines) and experiments (symbols) at 40 kW/m^2 at different oxygen concentrations. The solid lines indicate the average predictions, and the two dashed black lines the variability (twice the standard deviation) in the predictions due to the variability in chemical composition.

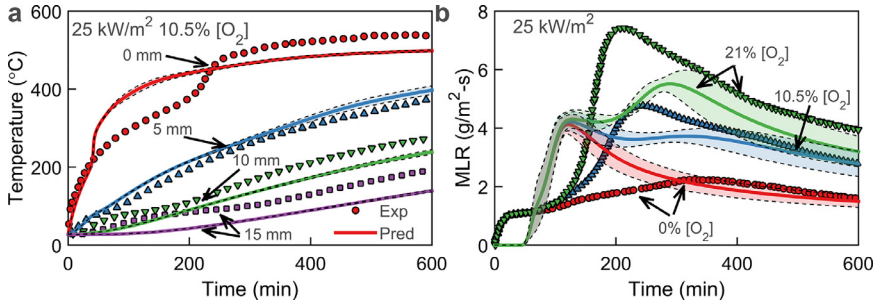

Fig. 8. Comparison between predictions and experiments at an external heat flux of 25 kW/m^2. The solid lines indicate the average predictions, and the two dashed black lines the variability (twice the standard deviation) in the predictions due to the variability in chemical composition.

crepancy. The missing fuel oxidation reactions of wood are the likely cause of the disagreement, as supported by Anca-Couce et al. [13,22]. The chosen kinetics and experiments at the microscale focussed on inert experiments [8] and revisiting them for oxidative environments should improve the agreement. Nevertheless, we judged the model as appropriate for this study for two reasons: Firstly, the agreement represents the quality of current state-of-the-art condense-phase fire models in blind predictions [22]. Posterior calibration (not conducted here) would have significantly improved the agreement. Secondly, charring rates, and so the decay of loadbearing capacity, of timber are derived from the temperature profiles, which are well predicted.

The composition has little effect, maximum deviation ±8 K, on the surface temperature (Fig. 7a–c), as it is controlled by heat transfer [22]. For the

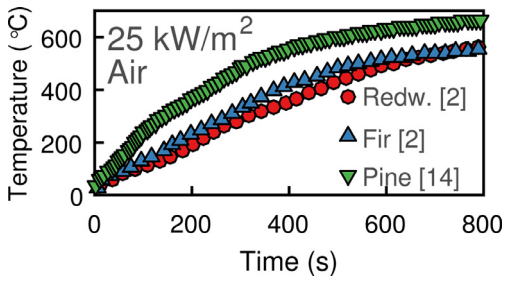

Fig. 9. Experimental temperature at 4 (redwood and fir) and 5 (pine) mm at 25 kW/m^2 of different species.

in-depth temperatures the effect of chemical composition becomes more significant with time under all conditions (maximum ±16 K at 600 s, Fig. 7c). As all predications only vary in composition (same material properties and heat of pyrolysis), the variation in temperature with time is caused by the different char yields of different species—the only parameter left linking heat transfer and kinetics. Varying the composition varies the total char yield, as each component yields different amounts of char. In turn, that varies the heat transfer to the intact wood and the heat release by oxidation. The small variation in temperature under inert environment (Fig. 7a), makes the different heat release by oxidation the most likely cause for the variation in temperature in reactive environment.

Similarly, the composition has little effect on the initial peak at 40 s in Fig. 7d and at 80 s in 8b in the mass loss rate. With time, the mass loss rate varies more significantly between species (up to ±1 g/m^2-s). This range is negligible for charring, but potentially not for other fire phenomena. For example, a critical mass loss rate is often used to assess if flaming ignition and self-extinction of timber occurred. The variation (±1 g/m^2-s) is of the same magnitude as the critical mass loss rate (3–10 g/m^2-s) [10,23]. Hence, ignition and self-extinction could be affected although this aspect is outside the scope of this paper. The same conclusions hold true for the case of 25 kW/m^2.

The measured temperatures at depths of 4 to 5 mm of several softwoods by [2,14] under similar moisture contents reveal a small difference between species at the same depth (average deviation: ± 22 K) (Fig. 9). Shen et al. [24] also found small differences (±34 K at 20 kW/m^2) in the surface temperatures between different hardwoods, meaning that our results are consistent with experimental findings.

The residual loadbearing capacity of timber sections at the macroscale (for buildings) is calculated from charring rates [1] which are determined from mesoscale experiments or models. The results from the mesoscale model should, therefore, apply directly to the marcoscale. Hence, the variation in kinetics within softwood is negligible for charring of structural softwood (timber). Our results from the microscale and other literature studies suggest that the same conclusions would hold for hardwood.

The main limitation of this work is that we only studied one reaction scheme in detail. The results, however, are applicable to all reaction schemes with several fuel components that degrade independently. All current state-of-the-art-models [7–9,25] belong to this group. For example, the propagation of the variation in species through the most complex of these kinetic models, the Ranzi scheme [9] without secondary reactions, leads to the same conclusions (see supplementary materials Fig S2) as earlier in Section 3.2 (Fig. 6). Hence, there is sufficient evidence to conclude that our results hold in general.

4. Conclusion

In this paper, we tested the hypothesis that the kinetics of different wood species insignificantly affects the charring of wood. Based on over 600 collected chemical compositions, we found that the variation of cellulose, hemicellulose, and lignin is small within softwood (timber) and hardwood. At the microscale, the variation proved to be insignificant to predict the rate of degradation. The peak reaction rate only varies by 22% which is reasonable compared to a 12% experimental uncertainty. The corresponding temperature remains constant. Notably, this analysis shows the uncertainty of choosing the kinetics of timber a priori to knowing the exact species, which is an expected scenario in professional practice. At the mesoscale, the difference in kinetics, including both pyrolysis and char oxidation reactions, proved insignificant for temperature and mass loss rate predictions for the charring of wood, but potentially significant for other fire phenomena. The predicted temperatures and mass loss rates vary by at most ±16 K and ±1 g/m^2-s, indicating that the influence of kinetics reduces with the increase in scale from microscale to mesoscale. It is, therefore, reasonable to expect that the prediction of charring at the macroscale, i.e. structural members, is unaffected by variation in kinetics within timber. Consequently, the current kinetic models for charring of hardwood or softwood of one species are appropriate for all species. Modellers should, therefore, focus on the difference in material properties between different wood species. This conclusion validates the current practice and research methodology in fire protection engineering and fire science respectively.

Acknowledgment

We are grateful for the financial support of EPSRC, Arup, and the SFPE Foundation Award.

We like to thank all Imperial Hazelab members for their helpful comments. Data supporting this publication can be obtained from https://zenodo.org/collection/user-imperialhazelab.

Supplementary materials

Supplementary material associated with this article can be found, in the online version, at doi:10.1016/j.proci.2018.06.080.

References

[1] S. Deeny, R.M. Hadden, A. Lawrence, B. Lane, *Struct. Eng.* (2017).
[2] M.J. Spearpoint, J.G. Quintiere, *Combust. Flame* 123 (2000) 308–325.
[3] C. Lautenberger, C. Fernandez-Pello, *Combust. Flame* 156 (2009) 1503–1513.
[4] W.C. Park, A. Atreya, H.R. Baum, *Proc. Combust. Inst.* 32 (2009) 2471–2479.
[5] N. Boonmee, J.G. Quintiere, *Proc. Combust. Inst.* 30 (2005) 2303–2310.
[6] A. Atreya, *Pyrolysis, Ignition and Fire Spread on Horizontal Surfaces of Wood*, Harvard University, 1983.
[7] M. Müller-Hagedorn, H. Bockhorn, L. Krebs, U. Müller, *Proc. Combust. Inst.* 29 (2002) 399–406.
[8] R.S. Miller, J. Bellan, *Combust. Sci. Technol* 126 (1997) 97–137.
[9] P.E.A. Debiagi, C. Pecchi, G. Gentile, et al., *Energy & Fuels* 29 (2015) 6544–6555.
[10] I. Vermesi, M.J. DiDomizio, F. Richter, E.J. Weckman, G. Rein, *Fire Saf. J.* 91 (2017) 218–225.
[11] T.J. Ohlemiller, T. Kashiwagi, K. Werner, *Combust. Flame* 69 (1987) 155–170.
[12] T. Kashiwagi, H. Nambu, *Combust. Flame* 88 (1992) 345–368.
[13] A. Anca-Couce, N. Zobel, A. Berger, F. Behrendt, *Combust. Flame* 159 (2012) 1708–1719.
[14] T. Kashiwagi, T.J. Ohlemiller, K. Werner, *Combust. Flame* 69 (1987) 331–345.
[15] X. Huang, K. Li, H. Zhang, *Proc. Combust. Inst.* 36 (2017) 3167–3175.
[16] X. Huang, G. Rein, H. Chen, *Proc. Combust. Inst.* 35 (2015) 2673–2681.
[17] A. Anca-Couce, I. Obernberger, *Fuel* 167 (2016) 158–167.
[18] Energy research Centre of the Netherlands, Phyllis2-Database, 2017 <http://www.ecn.nl/phyllis2>.
[19] K. Raveendran, A. Ganesh, K.C. Khilar, *Fuel* 75 (1996) 987–998.
[20] M.G. Grønli, G. Varhegyi, C. Di Blasi, G. Várhegyi, C. Di Blasi, *Ind. Eng. Chem. Res.* 41 (2002) 4201–4208.
[21] P. Reszka, *In-Depth Temperature Profiles in Pyrolyzing Wood*, University of Edinburgh, 2008.
[22] N. Bal, G. Rein, *Fire Saf. J.* 61 (2013) 36–44.
[23] R. Emberley, A. Inghelbrecht, Z. Yu, J.L. Torero, *Proc. Combust. Inst.* 36 (2017) 3055–3062.
[24] D.K. Shen, S. Gu, K.H. Luo, A.V. Bridgwater, M.X. Fang, *Fuel* 88 (2009) 1024–1030.
[25] W.C. Park, A. Atreya, H.R. Baum, *Combust. Flame* 157 (2010) 481–494.